CHEMMEDCHEM

DOI: 10.1002/cmdc.200700205

Sila-Haloperidol, a Silicon Analogue of the Dopamine (D_2) Receptor Antagonist Haloperidol: Synthesis, Pharmacological Properties, and Metabolic Fate

Reinhold Tacke,*[a] Friedrich Popp,[a] Barbara Müller,[a] Bastian Theis,[a] Christian Burschka,[a] Alexandra Hamacher,[b] Matthias U. Kassack,[b] Dirk Schepmann,[c] Bernhard Wünsch,[c] Ulrik Jurva,[d] and Eric Wellner[d]

*Haloperidol (**1 a**), a dopamine (D_2) receptor antagonist, is in clinical use as an antipsychotic agent. Carbon/silicon exchange (sila-substitution) at the 4-position of the piperidine ring of **1 a** ($R_3COH \rightarrow R_3SiOH$) leads to sila-haloperidol (**1 b**). Sila-haloperidol was synthesized in a new multistep synthesis, starting from tetramethoxysilane and taking advantage of the properties of the 2,4,6-trimethoxyphenyl unit as a unique protecting group for silicon. The pharmacological profiles of the C/Si analogues **1 a** and **1 b** were studied in competitive receptor binding assays at D_1–D_5, σ_1, and σ_2 receptors. Sila-haloperidol (**1 b**) exhibits significantly different receptor subtype selectivities from haloperidol (**1 a**) at both receptor families. The C/Si analogues **1 a** and **1 b** were also studied for 1) their physicochemical properties (log D, pK_a, solubility in HBSS buffer (pH 7.4)), 2) their permeability in a human Caco-2 model, 3) their pharmacokinetic profiles in human and rat liver microsomes, and 4) their inhibition of the five major cytochrome P450 isoforms. In addition, the major in vitro metabolites of sila-haloperidol (**1 b**) in human liver microsomes were identified using mass-spectrometric techniques. Due to the special chemical properties of silicon, the metabolic fates of the C/Si analogues **1 a** and **1 b** are totally different.*

Introduction

Haloperidol (**1 a**) has remained one of the most widely used antipsychotics for the treatment of neuropsychiatric disorders such as schizophrenia since its development in the late 1950s,[1] due mainly to its efficacy in alleviating the positive symptoms (e.g. hallucination and delusion) of such diseases.[2] The unfortunate short- and irreversible long-term extrapyramidal side effects (EPSs), including Parkinsonism-like tardive dyskinesia, present a drawback, particularly in lengthy therapies with haloperidol (**1 a**), and have motivated the search for haloperidol analogues and other "atypical" antipsychotics that exhibit fewer EPSs.[3] With these considerations in mind, we examined the biological effects of sila-substitution (C/Si exchange)[4] of haloperidol (**1 a**) and thus synthesized its silicon analogue, sila-haloperidol (**1 b**),[5] whereby the R_3COH carbon atom in the piperidine ring was replaced by a silicon atom. In context with our systematic research on silicon-based drugs,[6] we carried out a full characterization of **1 b**·HCl (solution NMR studies, crystal structure analysis, ESI-MS studies of aqueous solutions) complemented by radioligand binding studies on hD_1, hD_2, hD_4, and hD_5 human dopamine receptors at that time.

In the original synthesis of **1 b**, certain selectivity problems were encountered during the last step, resulting in a somewhat low yield for the final deprotection (selective cleavage of only one of the two Si–C(phenyl) bonds) to the silanol. Herein

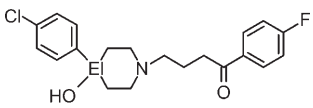

El = C: Haloperidol (**1a**)
El = Si: Sila-haloperidol (**1b**)

we report a new synthesis of **1 b** in which we took advantage of the special properties of the 2,4,6-trimethoxyphenyl unit as a protecting group for silicon[7] to achieve a more mild and se-

[a] *Prof. Dr. R. Tacke, F. Popp, B. Müller, B. Theis, Dr. C. Burschka*
Universität Würzburg, Institut für Anorganische Chemie
Am Hubland, 97074 Würzburg (Germany)
Fax: (+49) 931-888-4609
E-mail: r.tacke@mail.uni-wuerzburg.de

[b] *A. Hamacher, Prof. Dr. M. U. Kassack*
Universität Düsseldorf, Pharmazeutische und Medizinische Chemie
Geb. 26.23.01, Universitätsstrasse 1, 40225 Düsseldorf (Germany)

[c] *D. Schepmann, Prof. Dr. B. Wünsch*
Universität Münster, Institut für Pharmazeutische und Medizinische Chemie
Hittorfstrasse 58–62, 48149 Münster (Germany)

[d] *Dr. U. Jurva, Dr. E. Wellner*
AstraZeneca R&D Mölndal, Pepparedsleden 1, 43183 Mölndal (Sweden)

Supporting information for this article is available on the WWW under http://www.chemmedchem.org or from the author.

lective cleavage of the protecting group in the presence of other Si–C bonds.

In addition, we also present the missing pharmacological data for the hD_3 receptor, and we reinvestigated the affinities of **1a** and **1b** for all the other human dopamine receptors. As the antipsychotic effect of haloperidol (**1a**) is supported by its interaction with σ receptors,[8] and selective σ receptor antagonists are considered "atypical" antipsychotics,[9] the σ_1 and σ_2 receptor affinities of the C/Si analogues **1a** and **1b** were also studied. In addition to their in vitro pharmacodynamic properties, we also studied some physicochemical properties (log *D*, pK_a, solubility in HBSS buffer (pH 7.4)), the permeability in a human Caco-2 model, and the pharmacokinetic profiles (intrinsic clearance in human and rat liver microsomes) of haloperidol (**1a**) and sila-haloperidol (**1b**). Because inhibition of CYP450 enzymes is responsible for many severe side effects of drugs, the IC_{50} values of **1a** and **1b** for the five major CYP isoforms were measured as well. As one of the metabolites of haloperidol (**1a**) has been speculated to be responsible for the long-term, irreversible Parkinsonism-like side effects of this drug,[3] we were also interested in the metabolic fate of sila-haloperidol (**1b**) and performed comparative in vitro studies of the metabolism of the C/Si analogues **1a** and **1b** using human liver microsomes. This broad spectrum of studies aimed at a representative assessment of the potential of the carbon/silicon switch strategy[4,6] for drug design.

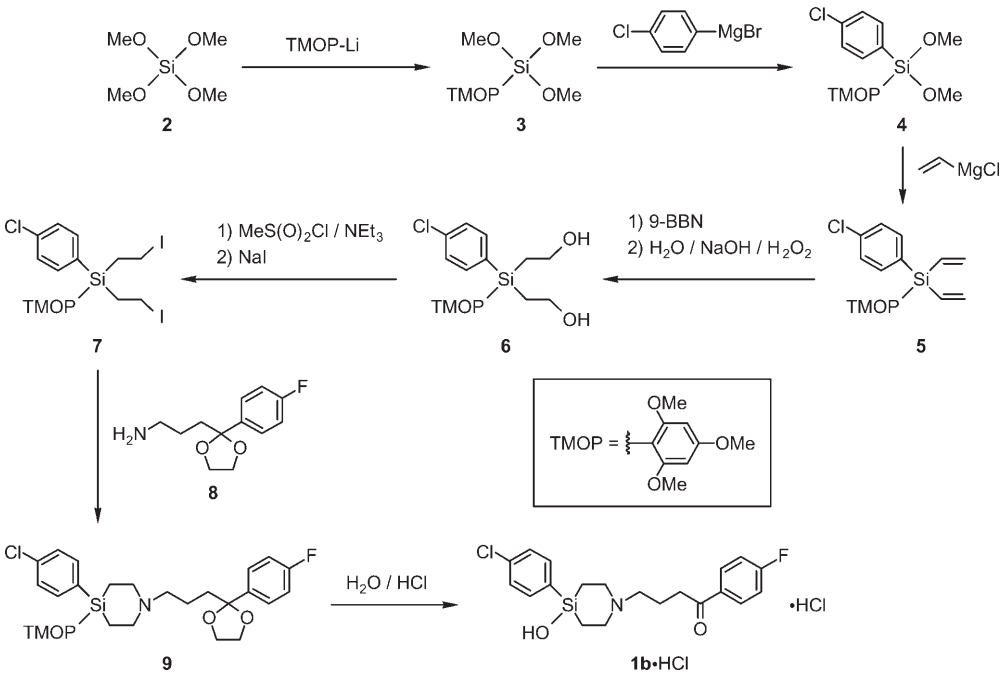

Scheme 1. Synthesis of sila-haloperidol hydrochloride (**1b**·HCl).

In addition to the carbon/silicon switch strategy, it should be mentioned that there are also other ways of applying organosilicon chemistry to drug design. Another innovative approach is the development of silicon-based drugs, the carbon analogues of which do not exist (for recent examples, see reference [10]). This strategy is also very versatile, as it has the potential to create new silicon-based drugs with structural motifs that would be chemically impossible for carbon-based drugs.

Results and Discussion

Syntheses

Sila-haloperidol (**1b**) was synthesized in a multistep synthesis starting from tetramethoxysilane (**2**) and was isolated as the hydrochloride **1b**·HCl (Scheme 1). Reaction of **2** with (2,4,6-trimethoxyphenyl)lithium gave the (2,4,6-trimethoxyphenyl)silane **3** (61% yield), which upon treatment with (4-chlorophenyl)-magnesium bromide afforded the (4-chlorophenyl)silane **4** (29% yield).[11] The reaction of **4** with vinylmagnesium chloride gave the divinylsilane **5** (63% yield). The aforementioned synthetic steps can also be performed starting with **2**, and without extensive purification of the intermediates **3** and **4**, to give **5** in 34% overall yield. This compares very favorably to the 11% overall yield with isolation of the intermediates. Compound **5** was then treated with 9-borabicyclo[3.3.1]nonane (9-BBN), followed by sequential treatment with aqueous solutions of sodium hydroxide and hydrogen peroxide, to give the bis(2-hydroxyethyl)silane **6** (69% yield). Reaction of **6** with methanesulfonyl chloride in the presence of triethylamine, followed by the addition of sodium iodide, afforded the bis(2-iodoethyl)silane **7** (81% yield). Treatment of **7** with 3-[2-(4-fluorophenyl)-1,3-dioxolan-2-yl]propylamine[12] (**8**) gave the cyclization product, the 4-silapiperidine **9** (50% yield). Deprotection of **9** by treatment with hydrochloric acid afforded the title compound as the hydrochloride (sila-haloperidol hydrochloride, **1b**·HCl, 71% yield). The identities of **1b**·HCl, **3**–**7**, and **9** were established by elemental analyses (C, H, N) and NMR studies (^1H, ^{13}C, ^{19}F, ^{29}Si). Compounds **5** and **6** were additionally characterized by single-crystal X-ray diffraction.

The selectivity problems encountered during the final deprotection step (selective cleavage of only one of the two Si–C(phenyl) bonds) with trifluoromethanesulfonic acid in the first synthesis of **1b**·HCl[5] have been solved by the use of the 2,4,6-trimethoxyphenyl group. Compared with the original synthesis, the deprotection reported herein is carried out in a single simple step under mild conditions with diluted hydrochloric acid to give the final product in well over twice the yield (71% vs. 30%). Due to this success, and because it fulfills the requirements demanded of a good protecting group in general,[13] we believe the 2,4,6-trimethoxyphenyl group indeed rep-

resents a particularly useful addition to the synthetic toolbox of the organosilicon chemist.

Receptor binding studies

The affinities of haloperidol (**1a**) and sila-haloperidol (**1b**) were studied at all human dopamine receptors. Table 1 presents the K_i values of **1a** and **1b** obtained in these studies. Hill slopes were not significantly different from unity, thus assuming a single binding site for **1a** and **1b** at all receptors. Affinities at the hD_1, hD_2, hD_4, and hD_5 receptors were similar to those previously reported.[5] Additionally, affinity data for the hD_3 receptor are presented. Figure 1 displays the competition binding curves of **1a** and **1b** at the hD_2 (Figure 1A) and hD_3 (Figure 1B) receptors. Whereas sila-haloperidol (**1b**) shows a significantly higher affinity for hD_2 receptors than haloperidol (**1a**) (5.1-fold), the silicon compound **1b** is approximately equipotent to its carbon analogue **1a** at all other dopamine receptors (differences are less than 2.3-fold).

Table 1. Affinities of **1a** and **1b** at human dopamine receptors.

Receptor subtype	K_i [nM][a]	
	1a	**1b**
hD_1	107 ± 22.0	162 ± 34.5
hD_2	2.84 ± 0.26	0.55 ± 0.06
hD_3	10.4 ± 1.47	4.73 ± 0.51
hD_4	7.94 ± 0.69	14.1 ± 1.09
hD_5	38.0 ± 4.72	16.6 ± 3.20

[a] Values are expressed as mean ± SEM from two experiments carried out in triplicate (except data for hD_4 and hD_5 receptors, which were obtained in one experiment with three replicates). All Hill slopes were not significantly different from unity.

The subtype selectivity of **1b** for hD_2 over the other dopamine receptors is somewhat higher than that of **1a** (Table 2). Sila-haloperidol (**1b**) has an approximately twofold higher selectivity than haloperidol (**1a**) for D_2 over D_3 and for D_2 over D_5 but an eight- to ninefold higher selectivity for D_2 over D_1 and for D_2 over D_4 relative to **1a**. The silicon compound **1b** thus has a different dopamine receptor subtype selectivity profile from its carbon analogue **1a**.

The σ_1 (guinea pig brain) and σ_2 (rat liver) receptor affinities of haloperidol (**1a**) and sila-haloperidol (**1b**) are given in Table 3. The K_i values of **1a** and **1b** at the σ_1 receptor are very similar and are in accordance with the reported σ_1 receptor affinity of **1a**.[14] At the σ_1 receptor, the C/Si analogues **1a** and **1b** are approximately equipotent.

In Figure 2, the competition binding curves of **1a** and **1b** at the σ_2 receptor are presented. Haloperidol (**1a**) exhibits threefold higher affinity for the σ_2 receptor than sila-haloperidol (**1b**). The reason for the lower affinity of **1b** for the σ_2 receptor is unclear. However, one might speculate that the carbon/silicon switch increases the distance between the σ_2 pharmacophoric elements (4-chlorophenyl ring and nitrogen atom) leading to decreased σ_2 affinity. On the other hand, the σ_1 receptor tolerates the structural modification and thus interacts with **1a** and **1b** with similar affinity. This observation is in accordance with the σ_1 pharmacophore model reported earlier.[15] Hence,

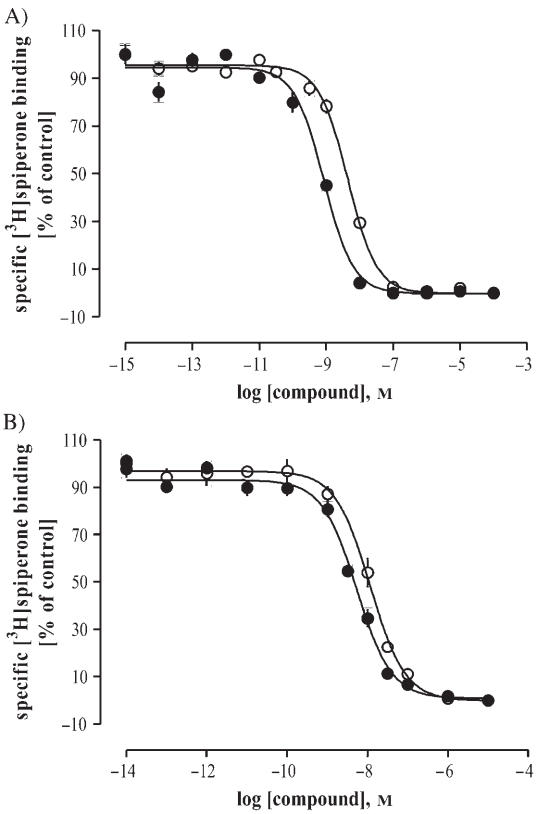

Figure 1. Competition binding curves resulting from the interaction of **1a** (○) and **1b** (●) with A) hD_2 and B) hD_3 dopamine receptors. Data are the means ± SEM of two experiments performed in triplicate. Slopes are not significantly different from unity.

Table 2. Selectivity of **1a** and **1b** for hD_2 over the other dopamine receptor subtypes.

Receptor subtypes	K_i value ratios	
	1a	**1b**
hD_1/hD_2	38	293
hD_3/hD_2	3.7	8.6
hD_4/hD_2	2.8	26
hD_5/hD_2	14	30

Table 3. Affinities of **1a** and **1b** at σ_1 receptors (guinea pig brain) and σ_2 receptors (rat liver).[a]

Receptor subtype	**1a**		**1b**	
	K_i [nM]	n_H	K_i [nM]	n_H
σ_1	1.9 ± 0.4	−1.43 ± 0.22	3.4 ± 0.4	−1.66 ± 0.93
σ_2	78.1 ± 2.4	−0.95 ± 0.25	309 ± 55	−0.89 ± 0.37

[a] K_i values and Hill slopes (n_H) are expressed as mean ± SEM from three experiments carried out in triplicate (except data for **1b** at the σ_2 receptor, the data for which were obtained in two experiments with three replicates).

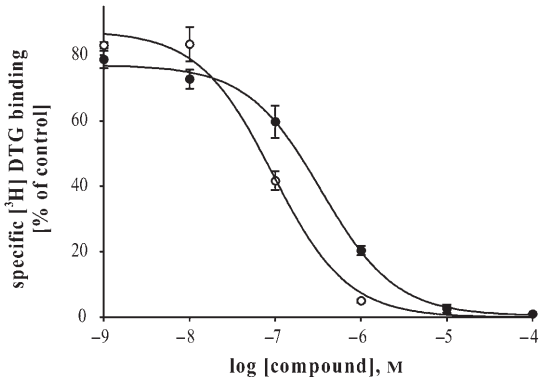

Figure 2. Competition binding curves resulting from the interaction of **1 a** (○) and **1 b** (●) with the σ_2 receptor. Data are the means ± SEM of two (**1 a**) or three (**1 b**) experiments performed in triplicate. Slopes are not significantly different from unity.

the subtype selectivity of sila-haloperidol (**1 b**) for the σ_1 receptor over the σ_2 receptor is approximately threefold higher than that of haloperidol (**1 a**).

In summary, in comparison with haloperidol (**1 a**), the silicon analogue sila-haloperidol (**1 b**) exhibits higher subtype selectivity at dopamine receptors as well as at σ receptors. These results once again demonstrate that the carbon/silicon switch strategy is a powerful tool to alter the pharmacodynamic properties of drugs.

Determination of physicochemical properties

To obtain information about the physicochemical properties of haloperidol (**1 a**) and sila-haloperidol (**1 b**), both compounds were studied as hydrochlorides for their octanol/water (pH 7.4) distribution coefficient (log *D* value), dissociation constant in water (pK_a value), and solubility in HBSS buffer (pH 7.4). As can be seen from Table 4, the respective data for the C/Si analogues **1 a** and **1 b** are each within the same range, indicating that the increased size and the decreased electronegativity of the silicon atom have no major effect on the overall physicochemical profile.

Table 4. Physicochemical properties of **1 a** and **1 b**.

Compound	log *D*[a]	pK_a[b]	Solubility [μM][c]
1 a	2.42 ± 0.03	9.07 ± 0.07	90 ± 2
1 b	2.77 ± 0.13	9.27 ± 0.10	78 ± 7

[a] Determined at pH 7.4; values represent the mean (n = 3). [b] Values represent the mean (n = 3). [c] Determined in HBSS buffer (pH 7.4); values represent the mean (n = 4).

Determination of permeability in a human Caco-2 model

To obtain information about their apparent permeability (P_{app}), haloperidol (**1 a**) and sila-haloperidol (**1 b**) were studied in a human Caco-2 model. In both cases, the apparent permeability was high (**1 a**, $P_{app} = 18.9 \times 10^{-6}$ cm s^{-1}; **1 b**, $P_{app} = 19.8 \times 10^{-6}$ cm s^{-1} for the unidirectional apical-to-basolateral (A to B) transport of the test compound). The recovery rate for **1 a** and **1 b** was around 90%, indicating that both compounds passed the cellular barrier more or less unchanged. Because haloperidol (**1 a**) is known to possess good bioavailability in humans,[16] these results suggest a high permeability for sila-haloperidol (**1 b**) as well.

Determination of intrinsic clearance and half-lives in liver microsomes

To determine the rate of decomposition of haloperidol (**1 a**) and sila-haloperidol (**1 b**) in vitro, the intrinsic clearance (CL_{int}) and half-lives ($t_{1/2}$) were measured in human and female rat liver microsomes (for a recent review dealing with in vitro estimation of metabolic stability, see reference [17]). As shown in Table 5, the C/Si analogues **1 a** and **1 b** showed a similar moderate stability in the presence of human liver microsomes. However, decomposition in the presence of rat liver microsomes was significantly increased by the carbon/silicon switch as can be observed from the half-lives of compounds **1 a** and **1 b** (**1 a**, $t_{1/2\,rat}$ = 65 min; **1 b**, $t_{1/2\,rat}$ = 18 min).

Table 5. Intrinsic clearance and half-life of **1 a** and **1 b** in human and rat liver microsomes.

Compd	$CL_{int\,hu}$ [μL min^{-1} mg^{-1}][a]	$CL_{int\,rat}$ [μL min^{-1} mg^{-1}][a]	$t_{1/2\,hu}$ [min]	$t_{1/2\,rat}$ [min]
1 a	20 ± 2	21 ± 5	51	65
1 b	21 ± 2	78 ± 7	65	18

[a] Values represent the mean (n = 4).

Determination of CYP inhibition

As haloperidol (**1 a**) and its metabolites are known to be strong cytochrome P450 (CYP) inhibitors,[21] it was also of great interest to investigate the CYP inhibition of sila-haloperidol (**1 b**) against the five major isoforms of CYP450 (Table 6). No CYP inhibition of either **1 a** or **1 b** against CYP2C9, CYP1A2, and CYP2C19 could be detected (> 20 μM). However, the silicon compound **1 b** revealed an almost threefold increased inhibito-

Table 6. CYP inhibition of **1 a** and **1 b**.

Compound	IC_{50} [μM]				
	CYP3A4[a]	CYP2C9[b]	CYP1A2[b]	CYP2C19[b]	CYP2D6[b]
1 a	26.2 ± 7.9	> 20	> 20	> 20	2.1 ± 0.6
1 b	9.6 ± 1.4	> 20	> 20	> 20	1.7 ± 0.9

[a] Values represent the mean (n = 6). [b] Values represent the mean (n=3).

ry effect (IC_{50} = 9.6 μM) against CYP3A4 relative to the parent carbon compound **1a** (IC_{50} = 26.2 μM). This change in activity might result from the altered ring conformation of sila-haloperidol (**1b**) due to the longer Si–C bonds (compared with the analogous C–C bonds), which might lead to increased CYP3A4 recognition. CYP2D6 was also inhibited by compounds **1a** and **1b**, with almost identical IC_{50} values (**1a**, 2.1 μM; **1b**, 1.7 μM). In this context it should be mentioned that the haloperidol (**1a**) metabolites HPTP and HPP^+ are believed to be strong CYP2D6 inhibitors.[18] As the sila-analogues of these metabolites, sila-HPTP and sila-HPP^+, are not formed (see next section), the possible interactions between sila-haloperidol (**1b**) and CYP2D6 substrates could be significantly altered relative to haloperidol (**1a**).

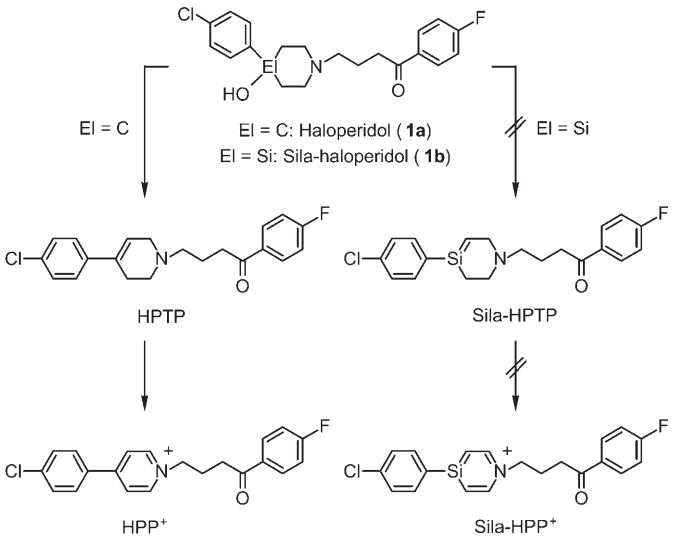

Scheme 2. Metabolism of haloperidol (**1a**): Formation of the neurotoxic pyridinium metabolite HPP^+ via the elimination product HPTP. The formation of sila-HPTP and sila-HPP^+ from sila-haloperidol (**1b**) is not possible.

Identification of the major in vitro metabolites of sila-haloperidol

It is known that one of the major metabolites of haloperidol[19] (**1a**), the 4-(4-chlorophenyl)-1-[4-(4-fluorophenyl)-4-oxobutyl]-pyridinium cation (HPP^+), has neurotoxic properties and is suspected to cause severe EPSs including Parkinsonism in patients on long-term haloperidol therapy.[20] The formation of HPP^+ is initiated by the generation of 4-(4-chlorophenyl)-1-[4-(4-fluorophenyl)-4-oxobutyl]-1,2,3,6-tetrahydropyridine (HPTP) caused by the acid-catalyzed[21] and/or enzyme-mediated[22] water elimination from haloperidol (**1a**) (Scheme 2). Analogous water elimination from sila-haloperidol (**1b**) under formation of the sila-HPTP analogue is not possible; due to the special chemical properties of silicon, a stable Si=C double bond will not be formed (Scheme 2). Consequently, the formation of neurotoxic pyridinium species (sila-HPP^+) in the case of sila-haloperidol (**1b**) is not possible.

In our efforts to identify the in vitro metabolites of sila-haloperidol (**1b**) in human liver microsomes, we observed the formation of three major metabolites (**M1**–**M3**) using mass-spectrometric techniques. The structures of the proposed metabolites are tentatively assigned based on accurate mass measurements and interpretation of MS–MS spectra. The *m/z* values observed, the retention times (t_R), as well as the estimated percentage of formation based on integration of extracted ion chromatograms are presented in Table 7.

The metabolite **M1** most likely originates from an oxidative N-dealkylation of **1b**, a process that is well known for the formation of haloperidol metabolites[23] (Scheme 3). Because the water elimination from **1b** to generate the corresponding sila-HPP^+ species is not possible, the silicon compound underwent an alternative metabolism to give the metabolites **M2** and **M3**. Upon oxidation of **1b**, the metabolite **M2** was probably formed by ring opening of the sila-piperidine skeleton due to an initially generated iminium intermediate[24] or a Peterson-like process with the loss of acetaldehyde. In a final step, **M2** underwent an intramolecular enamine formation to give **M3**.

In the case of haloperidol (**1a**), the major in vitro metabolite in human liver microsomes was HPP^+, using the same experimental conditions as for **1b**. Thus, as can be seen from the proposed metabolic pathways described in Scheme 3, the sila-analogue **1b** displayed a completely altered metabolic fate while otherwise maintaining a similar pharmacokinetic profile.

Conclusions

Sila-haloperidol (**1b**), a silicon analogue of the dopamine (D_2) antagonist haloperidol (**1a**), was prepared from tetramethoxysilane in a multistep synthesis and was isolated as the hydrochloride **1b**·HCl. In this synthesis, the use of the 2,4,6-trimethoxyphenyl moiety as a protecting group for silicon played a key role.

The pharmacodynamic profiles of the C/Si analogues **1a** and **1b** were studied in competitive receptor binding assays at D_1–D_5 (human), σ_1 (guinea pig brain), and σ_2 (rat liver) receptors. Both compounds showed no agonistic behavior at hD_1 and

Table 7. Sila-haloperidol (**1b**) metabolites after an incubation period of 60 min in human liver microsomes.

Metabolite	t_R [min]	*m/z* Values of protonated parent species	*m/z* Values of major MS–MS ions	Estimated formation [%]
1b	3.25	392.1238	392.1223, 394.1225, 165.0718, 164.0874, 123.0242	69
M1	1.52	228.0608	190.0091, 192.0064, 171.9982, 173.9953	8
M2	1.86	382.1038	382.1054, 384.1050, 172.9834, 174.9781, 165.0712, 164.0860, 123.0234	7
M3	2.45	364.0924	364.0931, 366.0930, 172.9821, 174.9792, 164.0866	12

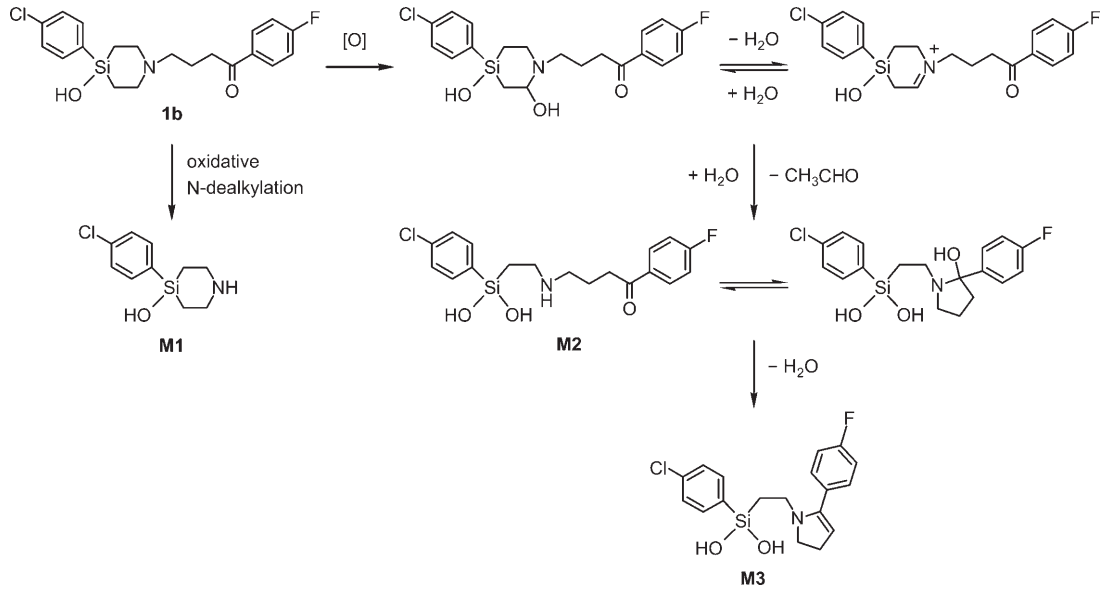

Scheme 3. Proposed metabolic pathways of sila-haloperidol (**1b**) in human liver microsomes. The structures of the proposed metabolites **M1**, **M2**, and **M3** are tentatively assigned based on accurate mass measurements and interpretation of MS–MS spectra.

hD_2 receptors in a functional calcium assay performed according to reference [25]. Whereas in receptor binding studies sila-haloperidol (**1b**) showed a significantly (fivefold) higher affinity for hD_2 receptors than haloperidol (**1a**), the silicon compound **1b** was approximately equipotent to its carbon analogue **1a** at all other dopamine receptors. Furthermore, the subtype selectivity for hD_2 over the other dopamine receptors was somewhat higher than that of **1a**. On the other hand, haloperidol (**1a**) showed a threefold higher affinity for the σ_2 receptor over sila-haloperidol (**1b**), whereas the σ_1 receptor tolerated the C/Si exchange and interacted with **1a** and **1b** with similar affinity. Hence, the subtype selectivity of the silicon compound **1b** for the σ_1 receptor over the σ_2 receptor is higher than that of the parent carbon compound **1a**. In summary, in comparison with haloperidol (**1a**), sila-haloperidol (**1b**) shows a higher potency at hD_2 receptors and exhibits a higher subtype selectivity at dopamine receptors and at σ receptors as well.

As shown for the log*D* and pK_a values and for the solubility in HBSS buffer (pH 7.4), the C/Si analogues **1a** and **1b** display a similar overall physicochemical profile (studies performed with **1a**·HCl and **1b**·HCl). The apparent permeability (P_{app}) of **1a** and **1b** was similar as well (human Caco-2 model). In both cases, the P_{app} values were high, and the recovery rate of both compounds was around 90%. Studies of the intrinsic clearance (CL_{int}) and half-life ($t_{1/2}$) in human liver microsomes revealed a similar moderate stability of **1a** and **1b**. However, decomposition in the presence of rat liver microsomes was significantly increased by the carbon/silicon switch. Haloperidol (**1a**) and sila-haloperidol (**1b**) showed no CYP inhibition against CYP2C9, CYP1A2, and CYP2C19. However, the silicon compound **1b** revealed an almost threefold increased inhibitory effect against CYP3A4 relative to the carbon analogue **1a**. CYP2D6 was also inhibited by **1a** and **1b**, with almost identical IC_{50} values.

As postulated earlier,[5a] the metabolic fate of the C/Si analogues **1a** and **1b** is totally different. Three major in vitro metabolites of sila-haloperidol (**1b**) in human liver microsomes could be observed using mass-spectrometric techniques. None of these metabolites represents a silicon analogue of the neurotoxic haloperidol (**1a**) metabolite, HPP^+, which is responsible for the severe side effects of **1a**.

In summary, sila-substitution at the 4-position of the piperidine ring of haloperidol (**1a**) significantly affects its pharmacological profile and metabolic fate in vitro. These results once again emphasize the great potential of the carbon/silicon switch strategy for drug design.

Experimental Section

Chemistry

General procedures: All syntheses were carried out under dry nitrogen. The organic solvents used were dried and purified according to standard procedures and stored under dry nitrogen. A Büchi GKR 50 apparatus was used for the bulb-to-bulb distillations. Melting points were determined with a Büchi Melting Point B-540 apparatus using samples in sealed glass capillaries. The ^{1}H, ^{13}C, ^{19}F, and ^{29}Si NMR spectra were recorded at 22 °C on a Bruker DRX-300 (^{1}H, 300.1 MHz; ^{13}C, 75.5 MHz; ^{29}Si, 59.6 MHz), a Bruker Avance 400 (^{1}H, 400.1 MHz; ^{13}C, 100.6 MHz; ^{19}F, 376.5 MHz; ^{29}Si, 79.5 MHz), or a Bruker Avance 500 NMR spectrometer (^{1}H, 500.1 MHz; ^{13}C, 125.8 MHz; ^{29}Si, 99.4 MHz). C_6D_6, $CDCl_3$, or [D_6]DMSO were used as the solvent. Chemical shifts (δ, ppm) were determined relative to internal C_6HD_5 [^{1}H: $\delta = 7.28$ ppm (C_6D_6)], C_6D_6 [^{13}C: $\delta = 128.0$ ppm (C_6D_6)], $CHCl_3$ [^{1}H: $\delta = 7.24$ ppm ($CDCl_3$)], $CDCl_3$ [^{13}C: $\delta = 77.0$ ppm ($CDCl_3$)], [D_5]DMSO [^{1}H: $\delta = 2.49$ ppm ([D_6]DMSO), [D_6]DMSO [^{13}C: $\delta = 39.5$ ppm ([D_6]DMSO), external $CFCl_3$ [^{19}F: $\delta = 0$ ppm (C_6D_6, $CDCl_3$, [D_6]DMSO)], or external TMS [^{29}Si: $\delta = 0$ ppm (C_6D_6, $CDCl_3$, [D_6]DMSO)]. Analysis and assignment of the ^{1}H NMR data was supported by ^{1}H,^{1}H gradient-selected COSY, ^{13}C,^{1}H gradient-selected

HMQC and gradient-selected HMBC, and ^{29}Si,^{1}H gradient-selected HMQC (optimized for $^{2}J_{SiH} = 7$ Hz). Assignment of the ^{13}C NMR data was supported by DEPT 135 and the aforementioned ^{13}C,^{1}H correlation experiments.

4-(4-Chlorophenyl)-4-hydroxy-1-[4-oxo-4-(4-fluorophenyl)butyl]-4-silapiperidinium chloride (1b·HCl): A solution of **9** (860 mg, 1.47 mmol) and 2 M aqueous solution of HCl (2.50 mL, 5.00 mmol of HCl) in acetone (10 mL) was heated under reflux for 3 h and thereafter stirred for a further 16 h at 20 °C. The reaction mixture was then added dropwise to Et_2O (60 mL), the resulting mixture was stirred for 10 min, and the precipitate was separated from the solution by centrifugation. The solid product was further purified through resuspension in Et_2O (25 mL), followed by centrifugation and drying in vacuo (0.01 mbar, 40 °C, 2 h) to give analytically pure **1b**·HCl in 71% yield as a colorless solid (444 mg, 1.04 mmol). The product may be recrystallized from 2-propanol/H_2O [1.5:1 (*v*/*v*)] to afford **1b**·HCl as a colorless crystalline solid in 59% yield; mp: 165 °C; ^{1}H NMR (500.1 MHz, [D_6]DMSO; data for two conformers): $\delta = 1.01$–1.10, 1.24–1.37, and 1.51–1.63 (m, 4H; $SiCH_2CH_2N$), 1.96–2.14 (m, 2H; $NCH_2CH_2CH_2C$), 3.06–3.45 and 3.52–3.70 (m, 8H; $SiCH_2CH_2N$, $NCH_2CH_2CH_2C$), 6.83 and 6.84 (s, 1H; SiO*H*), 7.31–7.41 (m, 2H; *H*-3/*H*-5, CC_6H_4F), 7.43–7.53 (m, 2H; *H*-3/*H*-5, SiC_6H_4Cl), 7.64–7.73 (m, 2H; *H*-2/*H*-6, SiC_6H_4Cl), 8.01–8.11 (m, 2H; *H*-2/*H*-6, CC_6H_4F), 10.7 and 10.9 ppm (br s, 1H; N*H*); ^{13}C NMR (125.8 MHz, [D_6]DMSO; data for two conformers, the dominating conformer marked with an asterisk, except for those signals that could not be resolved): $\delta = 9.5$ and 11.7* ($SiCH_2CH_2N$), 17.9* and 18.2 ($NCH_2CH_2CH_2C$), 35.1 and 35.3* ($NCH_2CH_2CH_2C$), 50.5 and 51.6* ($SiCH_2CH_2N$), 51.9 and 55.6* ($NCH_2CH_2CH_2C$), 115.7 (d, $^{2}J_{CF} = 21.8$ Hz, *C*-3/*C*-5, CC_6H_4F), 127.95* and 128.01 (*C*-3/*C*-5, SiC_6H_4Cl), 130.85 and 130.88* (d, $^{3}J_{CF} = 9.6$ Hz, *C*-2/*C*-6, CC_6H_4F), 133.2 (d, $^{4}J_{CF} = 2.6$ Hz, *C*-1, CC_6H_4F), 134.1 and 134.4* (*C*-1, SiC_6H_4Cl), 135.27* and 135.34 (*C*-4, SiC_6H_4Cl), 135.5* and 135.6 (*C*-2/*C*-6, SiC_6H_4Cl), 165.0 (d, $^{1}J_{CF} = 251.7$ Hz, *C*-4, CC_6H_4F), 197.3 ppm (*C*=O); ^{19}F NMR (376.5 MHz, [D_6]DMSO; data for two conformers, the dominating conformer marked with an asterisk): $\delta = -105.97$* and -105.96 ppm; ^{29}Si NMR (99.4 MHz, [D_6]DMSO; data for two conformers, the dominating conformer marked with an asterisk): $\delta = -10.9$* and -10.6 ppm; elemental analysis calcd (%) for $C_{20}H_{24}Cl_2FNO_2Si$ (428.4): C 56.07, H 5.65, N 3.27; found: C 55.8, H 5.6, N 3.1.

Tetramethoxysilane (2): This compound is commercially available (Sigma–Aldrich, Steinheim, Germany).

Trimethoxy(2,4,6-trimethoxyphenyl)silane (3): A 2.5 M solution of *n*-butyllithium in hexanes (125 mL, 313 mmol of *n*BuLi) was added dropwise at 20 °C within 60 min to a stirred solution of 1,3,5-trimethoxybenzene (50.8 g, 302 mmol) in a mixture of 1,2-bis(dimethylamino)ethane (TMEDA; 37.0 g, 318 mmol) and *n*-hexane (150 mL). The resulting suspension of (2,4,6-trimethoxyphenyl)lithium was stirred at 20 °C for a further 16 h and then added dropwise at 0 °C within 90 min to a stirred solution of **2** (46.4 g, 305 mmol) in Et_2O (150 mL). The reaction mixture was then stirred for 30 min at 0 °C and thereafter for 16 h at 20 °C. The precipitate was removed by filtration through a glass frit and washed with Et_2O (8×50 mL). The filtrate and wash solutions were combined, and the solvents were removed under reduced pressure. The resulting oily residue was purified by fractional distillation (bp: 145–149 °C at 0.01 mbar) to give **3** in 61% yield as a colorless viscous liquid (53.0 g, 184 mmol) that solidified after being left undisturbed for five days at 20 °C to give a colorless crystalline solid; mp: 32 °C; ^{1}H NMR (400.1 MHz, $CDCl_3$): $\delta = 3.57$ (s, 9H; $SiOCH_3$), 3.78 (s, 6H; *o*-OCH_3, $SiC_6H_2(OCH_3)_3$), 3.80 (s, 3H; *p*-OCH_3, $SiC_6H_2(OCH_3)_3$), 6.07 ppm (s, 2H; *H*-3/*H*-5, $SiC_6H_2(OCH_3)_3$); ^{13}C NMR (100.6 MHz, $CDCl_3$): $\delta = 50.7$ ($SiOCH_3$), 55.2 (*p*-OCH_3, $SiC_6H_2(OCH_3)_3$), 55.7 (*o*-OCH_3, $SiC_6H_2(OCH_3)_3$), 90.4 (*C*-3/*C*-5, $SiC_6H_2(OCH_3)_3$), 97.1 (*C*-1, $SiC_6H_2(OCH_3)_3$), 164.4 (*C*-4, $SiC_6H_2(OCH_3)_3$), 167.2 ppm (*C*-2/*C*-6, $SiC_6H_2(OCH_3)_3$); ^{29}Si NMR (79.5 MHz, $CDCl_3$): $\delta = -53.5$ ppm; elemental analysis calcd (%) for $C_{12}H_{20}O_6Si$ (288.4): C 49.98, H 6.99; found: C 49.9, H 6.7.

(4-Chlorophenyl)dimethoxy(2,4,6-trimethoxyphenyl)silane (4): A solution of (4-chlorophenyl)magnesium bromide prepared from 1-bromo-4-chlorobenzene (16.6 g, 86.7 mmol) and magnesium turnings (2.15 g, 88.5 mmol) in Et_2O (100 mL) was added dropwise at 0 °C within 2 h to a stirred solution of **3** (25.0 g, 86.7 mmol) in Et_2O (150 mL). After the addition was complete, the reaction mixture was allowed to warm to 20 °C and stirred at this temperature for a further 16 h. The precipitate was then removed by filtration through a glass frit and washed with Et_2O (3×100 mL). The filtrate and the wash solutions were combined, and the solvents were removed under reduced pressure. The resulting oily residue was purified by fractional distillation (Vigreux column; bp: 171–178 °C at 0.01 mbar) to give **4** in 29% yield[11] as a colorless viscous liquid (9.23 g, 25.0 mmol). ^{1}H NMR (300.1 MHz, $CDCl_3$): $\delta = 3.59$ (s, 6H; $SiOCH_3$), 3.65 (s, 6H; *o*-OCH_3, $SiC_6H_2(OCH_3)_3$), 3.81 (s, 3H; *p*-OCH_3, $SiC_6H_2(OCH_3)_3$), 6.07 (s, 2H; *H*-3/*H*-5, $SiC_6H_2(OCH_3)_3$), 7.25–7.31 (m, 2H; *H*-3/*H*-5, SiC_6H_4Cl), 7.50–7.57 ppm (m, 2H; *H*-2/*H*-6, SiC_6H_4Cl); ^{13}C NMR (75.5 MHz, $CDCl_3$): $\delta = 51.0$ ($SiOCH_3$), 55.2 (*p*-OCH_3, $SiC_6H_2(OCH_3)_3$), 55.5 (*o*-OCH_3, $SiC_6H_2(OCH_3)_3$), 90.6 (*C*-3/*C*-5, $SiC_6H_2(OCH_3)_3$), 99.0 (*C*-1, $SiC_6H_2(OCH_3)_3$), 127.5 (*C*-3/*C*-5, SiC_6H_4Cl), 134.4 (*C*-1, SiC_6H_4Cl), 135.4 (*C*-4, SiC_6H_4Cl), 135.5 (*C*-2/*C*-6, SiC_6H_4Cl), 164.6 (*C*-4, $SiC_6H_2(OCH_3)_3$), 167.2 ppm (*C*-2/*C*-6, $SiC_6H_2(OCH_3)_3$); ^{29}Si NMR (59.6 MHz, $CDCl_3$): $\delta = -28.9$ ppm; elemental analysis calcd (%) for $C_{17}H_{21}ClO_5Si$ (368.9): C 55.35, H 5.74; found: C 55.3, H 5.7.

(4-Chlorophenyl)(2,4,6-trimethoxyphenyl)divinylsilane (5). *Method A*: A solution of vinylmagnesium chloride (15 wt%, $d = 0.97$ g mL^{-1}; 33.0 mL, 55.3 mmol of CH_2=CHMgCl) in THF was added dropwise at 20 °C within 20 min to a stirred solution of **4** (9.20 g, 24.9 mmol) in THF (50 mL). After the addition was complete, the reaction mixture was heated under reflux for 30 min. The mixture was then allowed to cool to 20 °C and was subsequently treated with H_2O (50 mL). The aqueous layer was separated, diluted with H_2O (150 mL), and washed with Et_2O (3×100 mL). The organic layer and wash solutions were combined, washed with H_2O (50 mL), and dried over anhydrous Na_2SO_4. The organic solvents were removed under reduced pressure, leaving an oily residue that was purified by bulb-to-bulb distillation (150–155 °C at 0.01 mbar). The resulting solid was recrystallized from *n*-hexane at −20 °C to give **5** in 63% yield as a colorless crystalline solid (5.62 g, 15.6 mmol); mp: 56 °C; ^{1}H NMR (300.1 MHz, C_6D_6): $\delta = 3.25$ (s, 6H; *o*-OCH_3, $SiC_6H_2(OCH_3)_3$), 3.46 (s, 3H; *p*-OCH_3, $SiC_6H_2(OCH_3)_3$), 5.96 (δ_A), 6.28 (δ_M), and 6.94 (δ_X) (6H, CH_X=CH_AH_M, $^{3}J_{AX} = 20.3$ Hz, $^{2}J_{AM} = 3.8$ Hz, $^{3}J_{MX} = 14.4$ Hz), 6.13 (s, 2H; *H*-3/*H*-5, $SiC_6H_2(OCH_3)_3$), 7.31–7.37 (m, 2H; *H*-3/*H*-5, SiC_6H_4Cl), 7.63–7.68 ppm (m, 2H; *H*-2/*H*-6, SiC_6H_4Cl); ^{13}C NMR (75.5 MHz, C_6D_6): $\delta = 54.7$ (*o*-OCH_3 and *p*-OCH_3, $SiC_6H_2(OCH_3)_3$), 91.3 (*C*-3/*C*-5, $SiC_6H_2(OCH_3)_3$), 101.2 (*C*-1, $SiC_6H_2(OCH_3)_3$), 127.9 (*C*-3/*C*-5, SiC_6H_4Cl), 133.2 ($SiCH$=CH_2), 135.1 (*C*-1, SiC_6H_4Cl), 136.2 (*C*-4, SiC_6H_4Cl), 136.8 (*C*-2/*C*-6, SiC_6H_4Cl), 137.3 ($SiCH$=CH_2), 164.8 (*C*-4, $SiC_6H_2(OCH_3)_3$), 167.2 ppm (*C*-2/*C*-6, $SiC_6H_2(OCH_3)_3$); ^{29}Si NMR (59.6 MHz, C_6D_6): $\delta = -23.9$ ppm; elemental analysis calcd (%) for $C_{19}H_{21}ClO_3Si$ (360.9): C 63.23, H 5.86; found: C 63.1, H 5.9.

Method B: A 2.5 M solution of *n*-butyllithium in hexanes (121 mL, 303 mmol of *n*BuLi) was added dropwise at 20 °C within 60 min to a stirred solution of 1,3,5-trimethoxybenzene (50.0 g, 297 mmol) in a mixture of TMEDA (35.2 g, 303 mmol) and *n*-hexane (150 mL). The resulting suspension of (2,4,6-trimethoxyphenyl)lithium was

stirred at 20 °C for a further 3 h and then added dropwise at 0 °C within 100 min to a stirred solution of **2** (45.3 g, 298 mmol) in Et_2O (150 mL). The reaction mixture was then stirred for a further 60 min at 0 °C and thereafter for 16 h at 20 °C. The precipitate was removed by filtration through a glass frit and washed with Et_2O (4×100 mL). The filtrate and wash solutions were combined, and the solvents were removed under reduced pressure to give a viscous liquid (79.5 g), which was dissolved in Et_2O (500 mL). A solution of (4-chlorophenyl)magnesium bromide prepared from 1-bromo-4-chlorobenzene (51.7 g, 270 mmol) and magnesium turnings (6.90 g, 284 mmol) in Et_2O (300 mL) was then added dropwise within 2 h at 0 °C to this solution. After the addition was complete, the reaction mixture was allowed to warm to 20 °C and stirred for a further 16 h. The precipitate was then removed by filtration through a glass frit and washed with Et_2O (3×300 mL). The filtrate and wash solutions were combined and concentrated under reduced pressure to a volume of ca. 500 mL. A solution of vinylmagnesium chloride (15 wt%, $d = 0.97\ g\,mL^{-1}$; 370 mL, 620 mmol of $CH_2{=}CHMgCl$) in THF was then added dropwise at 20 °C within 2 h to this solution. After the addition was complete, the reaction mixture was heated under reflux for 3 h. The mixture was then allowed to cool to 20 °C and subsequently treated with H_2O (800 mL). The organic layer was separated and the aqueous layer washed with Et_2O (3×500 mL). The organic layer and wash solutions were combined, dried over anhydrous Na_2SO_4, and concentrated under reduced pressure. The resulting oily residue was purified by bulb-to-bulb distillation (140–170 °C at 0.01 mbar) to give a crystalline solid that was recrystallized from *n*-hexane at −20 °C to afford **5** in 34% overall yield as a colorless crystalline solid (33.4 g, 92.5 mmol); mp: 56 °C. The NMR data of the product were identical to those obtained for the product prepared by method A; elemental analysis calcd (%) for $C_{19}H_{21}ClO_3Si$ (360.9): C 63.23, H 5.86; found: C 63.1, H 5.8.

(4-Chlorophenyl)bis(2-hydroxyethyl)(2,4,6-trimethoxyphenyl)-silane (6): A solution of 9-borabicyclo[3.3.1]nonane (based on the 9-BBN dimer; 8.81 g, 36.1 mmol) and **5** (11.3 g, 31.3 mmol) in THF (220 mL) was stirred for 16 h at 20 °C. The reaction mixture was subsequently treated with H_2O (15.0 mL) and then with an aqueous solution of NaOH (3 M, 34.0 mL) at 20 °C. An aqueous solution of H_2O_2 (30 wt%, 34.0 mL) was then added dropwise within 15 min at 0 °C, after which the solution was heated under reflux for 2 h. After the reaction mixture had cooled to 20 °C, H_2O was added (150 mL), the organic layer was separated, and the aqueous layer was washed with CH_2Cl_2 (4×100 mL). The organic layer and wash solutions were combined and dried over anhydrous Na_2SO_4, and the organic solvents were removed under reduced pressure. The byproduct, cyclooctane-1,5-diol, was separated from the crude product by bulb-to-bulb distillation (150 °C at 0.01 mbar), and the residue was then crystallized from *n*-hexane/EtOAc/EtOH [5:2:1 (*v*/*v*/*v*)] using 5 mL solvent per 1 g crude product by slow cooling from reflux temperature to −20 °C to give **6** in 69% yield as a colorless crystalline solid (8.54 g, 21.5 mmol); mp: 114 °C; ^{1}H NMR (300.1 MHz, C_6D_6): $\delta = 1.62$–1.85 (m, 6H; SiCH_2CH_2OH), 3.19 (s, 6H; *o*-OCH_3, $SiC_6H_2(OCH_3)_3$), 3.45 (s, 3H; *p*-OCH_3, $SiC_6H_2(OCH_3)_3$), 3.82–3.97 (m, 4H, SiCH_2CH_2O), 6.08 (s, 2H; *H*-3/*H*-5, $SiC_6H_2(OCH_3)_3$), 7.30–7.36 (m, 2H; *H*-3/*H*-5, SiC_6H_4Cl), 7.46–7.52 ppm (m, 2H; *H*-2/*H*-6, SiC_6H_4Cl); ^{13}C NMR (75.5 MHz, C_6D_6): $\delta = 20.8$ (SiCH_2CH_2O), 54.6 (*o*-OCH_3 and *p*-OCH_3, $SiC_6H_2(OCH_3)_3$), 60.0 (SiCH_2CH_2O), 91.2 (*C*-3/*C*-5, $SiC_6H_2(OCH_3)_3$), 101.2 (*C*-1, $SiC_6H_2(OCH_3)_3$), 127.9 (*C*-3/*C*-5, SiC_6H_4Cl), 134.7 (*C*-1, SiC_6H_4Cl), 135.6 (*C*-2/*C*-6, SiC_6H_4Cl), 138.3 (*C*-4, SiC_6H_4Cl), 164.6 (*C*-4, $SiC_6H_2(OCH_3)_3$), 167.0 ppm (*C*-2/*C*-6, $SiC_6H_2(OCH_3)_3$); ^{29}Si NMR (59.6 MHz, C_6D_6): $\delta = -11.6$ ppm; elemental analysis calcd (%) for $C_{19}H_{25}ClO_5Si$ (396.9): C 57.49, H 6.35; found: C 57.4, H 6.2.

(4-Chlorophenyl)bis(2-iodoethyl)(2,4,6-trimethoxyphenyl)silane (7): A solution of methanesulfonyl chloride (3.66 g, 32.0 mmol) in CH_2Cl_2 (60 mL) was added dropwise at 20 °C (water bath cooling) within 30 min to a stirred solution of **6** (6.00 g, 15.1 mmol) and triethylamine (TEA; 15.4 g, 152 mmol) in CH_2Cl_2 (60 mL). After the addition was complete, the reaction mixture was stirred for a further 3 h at 20 °C. *n*-Pentane (150 mL) was subsequently added, and the precipitate was removed by filtration through a glass frit, washed with Et_2O (2×20 mL), and then discarded. The filtrate and wash solutions were combined, and the solvents were removed under reduced pressure. The resulting oily residue was dissolved in acetone (150 mL), and NaI (23.4 g, 156 mmol) was added in a single portion at 20 °C under exclusion of light. The reaction mixture was stirred for 1 h at 20 °C, *n*-hexane (60 mL) was added, and the mixture was stirred for an additional 16 h at 20 °C under exclusion of light. The solvents were subsequently removed under reduced pressure, and the resulting residue was treated with *n*-hexane (300 mL) and H_2O (400 mL). The organic layer was separated, and the aqueous layer was washed with *n*-hexane (4×200 mL). The organic layer and wash solutions were combined and dried over anhydrous Na_2SO_4, and the solvent was removed under reduced pressure. The residue was redissolved in *n*-hexane (200 mL), activated charcoal (1.00 g) was added, and the stirred mixture was heated at 50 °C for 30 min. The mixture was then allowed to cool to 20 °C, was filtered, and was finally cooled to −20 °C for 16 h under exclusion of light. The upper organic layer was separated with a syringe and discarded, and the liquid that had separated was freed of solvent in vacuo (0.01 mbar, 40 °C, 3 h) under exclusion of light to give **7** in 81% yield as a colorless and highly viscous liquid (7.52 g, 12.2 mmol). ^{1}H NMR (300.1 MHz, C_6D_6): $\delta = 1.89$–2.08 (m, 4H; $SiCH_2CH_2I$), 3.18 (s, 6H; *o*-OCH_3, $SiC_6H_2(OCH_3)_3$), 3.20–3.38 (m, 4H; SiCH_2CH_2I), 3.43 (s, 3H; *p*-OCH_3, $SiC_6H_2(OCH_3)_3$), 6.00 (s, 2H; *H*-3/*H*-5, $SiC_6H_2(OCH_3)_3$), 7.05–7.11 (m, 2H; *H*-2/*H*-6, SiC_6H_4Cl), 7.19–7.25 ppm (m, 2H; *H*-3/*H*-5, SiC_6H_4Cl); ^{13}C NMR (75.5 MHz, C_6D_6): $\delta = 3.0$ (SiCH_2CH_2I), 24.4 ($SiCH_2CH_2I$), 54.8 (*o*-OCH_3 and *p*-OCH_3, $SiC_6H_2(OCH_3)_3$), 91.0 (*C*-3/*C*-5, $SiC_6H_2(OCH_3)_3$), 97.9 (*C*-1, $SiC_6H_2(OCH_3)_3$), 128.3 (*C*-3/*C*-5, SiC_6H_4Cl), 134.9 (*C*-1, SiC_6H_4Cl), 135.2 (*C*-2/*C*-6, SiC_6H_4Cl), 135.5 (*C*-4, SiC_6H_4Cl), 165.1 (*C*-4, $SiC_6H_2(OCH_3)_3$), 167.0 ppm (*C*-2/*C*-6, $SiC_6H_2(OCH_3)_3$); ^{29}Si NMR (59.6 MHz, C_6D_6): $\delta = -10.2$ ppm; elemental analysis calcd (%) for $C_{19}H_{23}ClI_2O_3Si$ (616.7): C 37.00, H 3.76; found: C 37.5, H 4.5.[26]

3-[2-(4-Fluorophenyl)-1,3-dioxolan-2-yl]propylamine (8): This compound was synthesized according to reference [12].

4-(4-Chlorophenyl)-1-{3-[2-(4-fluorophenyl)-1,3-dioxolan-2-yl]-propyl}-4-(2,4,6-trimethoxyphenyl)-4-silapiperidine (9): Compound **8** (2.30 g, 10.2 mmol) was added to a stirred solution of **7** (6.00 g, 9.73 mmol) and TEA (2.96 g, 29.3 mmol) in CH_3CN (100 mL) at 20 °C. The reaction mixture was heated at 75 °C for 3 h and subsequently stirred at 20 °C for 16 h. The solvent and the excess TEA were then removed under reduced pressure, and the oily residue was treated with CH_2Cl_2 (100 mL) and H_2O (150 mL). The organic layer was separated, and the aqueous layer was washed with CH_2Cl_2 (2×100 mL). The organic layer and the wash solutions were combined and dried over anhydrous Na_2SO_4, and the solvent was removed under reduced pressure. The resulting oily residue was purified by column chromatography on Al_2O_3 (neutral, Type 507C, Brockmann I, 150 mesh, 58 Å; Aldrich cat. No. 199974; deactivated with 6 wt% H_2O) using a mixture of *n*-hexane/EtOAc [7:3 (*v*/*v*)] and 1% TEA as the eluent (product $R_f = 0.4$). The relevant fractions were combined, and the solvents were removed under reduced pressure. The residue was dissolved in *n*-hexane (40 mL) at reflux, and the resulting solution was subsequently cooled to −20 °C for 16 h. The upper organic layer was then separated with a syringe

and discarded, and the liquid that had separated was freed of solvent in vacuo (0.01 mbar, 70 °C, 3 h) to give **9** in 50% yield as a colorless and highly viscous liquid (2.86 g, 4.88 mmol). ^{1}H NMR (400.1 MHz, C_6D_6): δ = 1.61–1.71 and 1.74–1.84 (m, 4H; SiCH_2CH_2N), 1.85–1.95 (m, 2H; NCH$_2CH_2CH_2$C), 2.18–2.27 (m, 2H; NCH$_2CH_2CH_2$C), 2.51 (t, $^3J_{HH}$ = 7.0 Hz, 2H; N$CH_2CH_2CH_2$C), 2.76–2.87 and 3.06–3.16 (m, 4H; SiCH$_2CH_2$N), 3.29 (s, 6H; *o*-OCH_3, $SiC_6H_2(OCH_3)_3$), 3.41–3.50 (m, 5H; *p*-OCH_3, $SiC_6H_2(OCH_3)_3$, and CH_2OC), 3.61–3.71 (m, 2H; CH_2OC), 6.09 (s, 2H; *H*-3/*H*-5, $SiC_6H_2(OCH_3)_3$), 6.89–6.97 (m, 2H; *H*-3/*H*-5, CC_6H_4F), 7.31–7.37 (m, 2H; *H*-3/*H*-5, SiC_6H_4Cl), 7.48–7.55 (m, 2H; *H*-2/*H*-6, CC_6H_4F), 7.66–7.73 ppm (m, 2H; *H*-2/*H*-6, SiC_6H_4Cl); ^{13}C NMR (100.6 MHz, C_6D_6): δ = 14.8 (SiCH_2CH_2N), 22.5 (NCH$_2CH_2CH_2$C), 39.0 (NCH$_2CH_2CH_2$C), 53.4 (SiCH$_2CH_2$N), 54.66 (*o*-OCH_3, $SiC_6H_2(OCH_3)_3$), 54.70 (*p*-OCH_3, $SiC_6H_2(OCH_3)_3$), 58.7 (NCH$_2CH_2CH_2$C), 64.5 (CH_2OC), 90.9 (*C*-3/*C*-5, $SiC_6H_2(OCH_3)_3$), 102.5 (*C*-1, $SiC_6H_2(OCH_3)_3$), 110.5 (CH_2OC), 115.0 (d, $^2J_{CF}$ = 21.3 Hz, *C*-3/*C*-5, CC_6H_4F), 128.1 (d, $^3J_{CF}$ = 8.4 Hz, *C*-2/*C*-6, CC_6H_4F), 128.3 (*C*-3/*C*-5, SiC_6H_4Cl), 135.0 (*C*-1, SiC_6H_4Cl), 136.3 (*C*-2/*C*-6, SiC_6H_4Cl), 137.8 (*C*-4, SiC_6H_4Cl), 139.6 (d, $^4J_{CF}$ = 3.0 Hz, *C*-1, CC_6H_4F), 162.8 (d, $^1J_{CF}$ = 245.0 Hz, *C*-4, CC_6H_4F), 164.4 (*C*-4, $SiC_6H_2(OCH_3)_3$), 167.0 ppm (*C*-2/*C*-6, $SiC_6H_2(OCH_3)_3$); ^{19}F NMR (376.5 MHz, C_6D_6): δ = −115.0 ppm; ^{29}Si NMR (99.4 MHz, C_6D_6): δ = −17.4 ppm; elemental analysis calcd (%) for $C_{31}H_{37}ClFNO_5Si$ (586.2): C 63.52, H 6.36, N 2.39; found: C 63.1, H 6.2, N 2.3.

Crystal structure analyses: Suitable single crystals of **5** were obtained from a solution in *n*-pentane at 4 °C, and single crystals of **6** were obtained by evaporation of a saturated solution in Et_2O at 20 °C. The crystals were mounted in inert oil (perfluoroalkyl ether, ABCR) on a glass fiber and then transferred to the cold nitrogen gas stream of the diffractometer (Stoe IPDS; graphite-monochromated $Mo_{K\alpha}$ radiation (λ = 0.71073 Å)). The structures were solved by direct methods.[27] All non-hydrogen atoms were refined anisotropically.[28] A riding model was employed in the refinement of the C*H* hydrogen atoms. The O*H* hydrogen atoms of **6** were localized in difference Fourier syntheses and refined freely. For the results of these studies, see the Supporting Information.

Receptor binding studies at hD$_1$–hD$_5$ receptors

a) Materials: [^{3}H]SCH23390 (66 Ci mmol^{-1}) and [^{3}H]spiperone (118 Ci mmol^{-1}) were purchased from Nycomed Amersham (Buckinghamshire, UK). cDNA for the hD$_1$ and hD$_5$ dopamine receptors was kindly provided by Dr. D. Grandy (Portland, OR). A pcDNA vector construct for hD$_{2S}$ (short form) receptors was a gift from Dr. W. Sadée (San Francisco, CA). A pRc/CMV vector construct for hD$_3$ receptors was kindly provided by Dr. P. Sokoloff (Paris, France). The human D$_{4.4}$ receptor stably expressed in CHO cells was kindly provided by Dr. van Tol (Toronto, Canada). Compounds **1a** and **1b** were studied as hydrochlorides. All other reagents were supplied by Sigma Chemicals (Taufkirchen, Germany) unless otherwise stated.

b) Cell culture and transfection: HEK293 cells stably expressing hD$_1$, hD$_{2S}$, or hD$_5$ dopamine receptors[29,30] were grown in Dulbecco's modified Eagle's Medium Nutrient Mixture F-12 Ham (DMEM/F-12 1:1 mixture) containing fetal bovine serum (FBS, 10%), streptomycin (100 μg mL^{-1}), penicillin G (100 U mL^{-1}), L-glutamine (5 mM), and active G-418 (200 μg mL^{-1}). CHO cells stably expressing hD$_{4.4}$ dopamine receptors were grown in Ham F-12 medium supplemented with FBS (10%), streptomycin (100 μg mL^{-1}), penicillin G (100 U mL^{-1}), L-glutamine (1 mM), and active G-418 (200 μg mL^{-1}). Cells were incubated at 37 °C in a humidified atmosphere under 5% CO_2. HEK293 cells stably expressing hD$_3$ dopamine receptors were generated by transfecting the coding plasmid for hD$_3$ using polyfect transfection reagent (Qiagen, Hilden, Germany) according to the manufacturer's instructions. Stably transfected clones were selected using active G-418 (400 μg mL^{-1}).

c) Membrane preparations: Cells of confluent 145-mm tissue culture dishes (Greiner Bio-One, Frickenhausen, Germany) were harvested by scraping, resuspended in ice-cold Krebs-HEPES buffer (118 mM NaCl, 4.7 mM KCl, 1.2 mM $MgSO_4$, 1.2 mM KH_2PO_4, 4.2 mM $NaHCO_3$, 11.7 mM D-glucose, 1.3 mM $CaCl_2$, 10 mM HEPES, pH 7.4), and disrupted using a Polytron homogenizer on ice (Kinematica AG, Basel, Switzerland). After centrifugation at 40000 *g* at 2 °C, the supernatant was discarded, and the pellet was washed twice with ice-cold Krebs-HEPES buffer. Eventually, the pellet was resuspended in the appropriate binding buffer (see below) and stored in aliquots at −80 °C until use for radioligand binding.

d) Radioligand binding assays: The equilibrium dissociation constants K_d for [^{3}H]SCH23390 (hD$_1$, 1.93 nM; hD$_5$, 1.50 nM) and for [^{3}H]spiperone (hD$_2$, 0.18 nM; hD$_3$, 0.84 nM; hD$_4$, 0.30 nM) were determined in homologous competition binding experiments. The receptor densities of the respective dopamine receptor cell membrane preparations (B_{max} values: hD$_1$, 3520 fmol (mg protein)$^{-1}$; hD$_2$, 1641 fmol (mg protein)$^{-1}$; hD$_3$, 4060 fmol (mg protein)$^{-1}$; hD$_4$, 493 fmol (mg protein)$^{-1}$; hD$_5$, 1030 fmol (mg protein)$^{-1}$ were calculated using the DeBlasi equation.[31] Competition binding experiments with **1a** and **1b** were performed in total volumes of 1.1 mL at 26 °C for 2 h (D$_1$-like receptors) or 3 h (D$_2$-like receptors) with ca. 90 μg membrane protein in Krebs-HEPES buffer. For binding studies at hD$_1$-like receptors, [^{3}H]SCH23390 was used at a final concentration of 0.2 nM. At hD$_2$-like receptors, [^{3}H]spiperone was used at a final concentration of 0.1 nM. Nonspecific binding was defined as radioactivity bound in the presence of 1 μM LE300 (D$_1$-like receptors) or 1 μM haloperidol (D$_2$-like receptors) and was less than 10% of total binding. The assay was terminated by rapid filtration of 1 mL through polyethylenimine-pretreated (0.2%) glass fiber filters (Schleicher & Schuell, Dassel, Germany) followed by two washes with ice-cold distilled water. After adding 5 mL ReadyProtein (Beckman, Krefeld, Germany) and an incubation period of at least 12 h, radioactivity bound to the filters was quantified by liquid scintillation counting. The protein content of membrane preparations was determined by the method of Bradford[32] and bovine serum albumin (BSA) as the standard.

e) Data analysis: Binding data were analyzed by fitting the pooled data from two experiments carried out in triplicate (except data for hD$_4$ and hD$_5$, which were generated from one experiment in triplicate) to a four-parameter logistic equation using Prism software 3.0 (GraphPad Software; San Diego, CA, USA). Competition binding experiments were fitted best to a one-site binding model. Nonspecific binding was routinely subtracted. Inhibition constants K_i from radioligand binding competition experiments were calculated from IC_{50} values using the Cheng–Prusoff equation:[33]

$$K_i = IC_{50}/(1 + L/K_d) \quad (1)$$

where IC_{50} is the molar concentration of the test compound at half-maximum displacement of the radioligand, L is the molar concentration of the radioligand, and K_d is the equilibrium dissociation constant of the radioligand. Data (data points in the figures and numbers in the tables) are given as mean ± SEM from two independent experiments, each performed in triplicate unless otherwise stated.

Receptor binding studies at σ_1 and σ_2 receptors (modified according to references [34] and [35])

a) Materials and general procedures: The guinea pig brains and rat livers were commercially available (Harlan–Winkelmann, Borchen, Germany). Homogenizer: Elvehjem–Potter (B. Braun Biotech International, Melsungen, Germany); centrifuge: high-speed cooling centrifuge, model Sorvall RC-5C Plus (Thermo Scientific, Waltham, MA, USA); filter: printed Filtermat Type B (PerkinElmer, Waltham, MA, USA), presoaked in 0.5% aqueous polyethylenimine for 2 h at room temperature before use. The filtration was carried out with a MicroBeta FilterMate-96 harvester (PerkinElmer, Waltham, MA, USA). The scintillation analysis was performed using a Meltilex (Type A) solid scintillator (PerkinElmer, Waltham, MA, USA). The solid scintillator was melted on the filtermat at a temperature of 95 °C for 5 min. After solidification of the scintillator at room temperature, the scintillation was measured using a MicroBeta Trilux scintillation analyzer (PerkinElmer, Waltham, MA, USA). The counting efficiency was 40%.

b) Membrane preparation (σ_1 assay): Five guinea pig brains were homogenized (Elvehjem–Potter, 500–800 rpm, 10 up-and-down strokes) in six volumes of cold sucrose (0.32 M). The suspension was centrifuged at 1200 *g* for 10 min at 4 °C. The supernatant was separated and centrifuged at 23 500 *g* for 20 min at 4 °C. The pellet was resuspended in 5–6 volumes of buffer (50 mM Tris, pH 7.4) and centrifuged again at 23 500 *g* (20 min, 4 °C). This procedure was repeated twice. The final pellet was resuspended in 5–6 volumes of buffer, the protein concentration was determined according to the method of Bradford[32] using BSA as standard, and subsequently the preparation was frozen (−80 °C) in 1.5-mL portions containing ca. 1.5 (mg protein) mL^{-1}.

c) Membrane preparation (σ_2 assay): Two rat livers were cut into smaller pieces and homogenized (Elvehjem–Potter, 500–800 rpm, 10 up-and-down strokes) in six volumes of cold sucrose (0.32 M). The suspension was centrifuged at 1200 *g* for 10 min at 4 °C. The supernatant was separated and centrifuged at 31 000 *g* for 20 min at 4 °C. The pellet was resuspended in buffer (50 mM Tris, pH 8.0) and incubated at room temperature for 30 min. After the incubation, the suspension was centrifuged again at 31 000 *g* for 20 min at 4 °C. The final pellet was resuspended in buffer, the protein concentration was determined according to the method of Bradford[32] using BSA as standard, and subsequently the preparation was frozen (−80 °C) in 1.5-mL portions containing ca. 2 (mg protein) mL^{-1}.

d) Radioligand binding assay (σ_1). The test was performed with the radioligand [^{3}H](+)-pentazocine (42.5 Ci $mmol^{-1}$, PerkinElmer, Waltham, MA, USA). The thawed membrane preparation (ca. 75 μg of the protein) was incubated with various concentrations of test compound, [^{3}H](+)-pentazocine (2 nM), and buffer (50 mM Tris, pH 7.4) in a total volume of 200 μL for 180 min at 37 °C. The incubation was terminated by rapid filtration through the presoaked filtermats using a cell harvester. After washing each well with H_2O (5×300 μL), the filtermats were dried at 95 °C. Subsequently, the solid scintillator was placed on the filtermat and melted at 95 °C. After 5 min, the solid scintillator was allowed to solidify at room temperature. The bound radioactivity trapped on the filters was counted in the scintillation analyzer. The nonspecific binding was determined with unlabeled (+)-pentazocine (10 μM). The K_d value of the radioligand [^{3}H](+)-pentazocine is 2.9 nM.[14]

e) Radioligand binding assay (σ_2). The test was performed with the radioligand [^{3}H]ditolylguanidine (50 Ci $mmol^{-1}$, ARC, St. Louis, MO, USA). The thawed membrane preparation (ca. 100 μg of the protein) was incubated with various concentrations of test compound, [^{3}H]ditolylguanidine (3 nM), (+)-pentazocine (500 nM), and buffer (50 mM Tris, pH 8.0) in a total volume of 200 μL for 180 min at room temperature. The incubation was terminated by rapid filtration through the presoaked filtermats using a cell harvester. After washing each well with H_2O (5×300 μL), the filtermats were dried at 95 °C. Subsequently, the solid scintillator was placed on the filtermat and melted at 95 °C. After 5 min, the solid scintillator was allowed to solidify at room temperature. The bound radioactivity trapped on the filters was counted in the scintillation analyzer. The nonspecific binding was determined with unlabeled ditolylguanidine (10 μM). The K_d value of the radioligand [^{3}H]ditolylguanidine is 17.9 nM.[36]

f) Data analysis: All experiments were carried out in triplicate using standard 96-well multiplates (Diagonal, Münster, Germany). The IC_{50} values were determined in competition experiments with six concentrations of the test compounds and were calculated with the program GraphPad Prism 3.0 (GraphPad Software) by nonlinear regression analysis. K_i values were calculated according to Cheng and Prusoff.[33] Data (data points in the figures and numbers in the tables) are given as mean ±SEM from three independent experiments.

Determination of physicochemical properties

a) Materials: Hank's balanced saline solution (HBSS) and 2-[4-(2-hydroxyethyl)piperazino]ethanesulfonic acid (HEPES) were purchased from GIBCO (Carlsbad, CA, USA). The solvents used for the experiments were of analytical grade, and the water used was obtained from a water purification system (Elgastat Maxima, ELGA, Lane End, UK). The HBSS buffer (pH 7.4) was prepared as follows: An aqueous solution of HEPES (12.5 mL, 1 M) was added to 500 mL of HBSS, and the pH was adjusted to pH 7.4 by titration with an aqueous solution of NaOH (10 mM).

b) log *D* values: The log *D* values were obtained by determining the capacity factor *k'*: An Agilent 1100 HPLC system (Waldbronn, Germany) was used to inject samples onto a reversed-phase LC column (Waters XTerra C_{18}, 3.5 μm, 100×2.1 mm). The outlet from the LC column was connected to a Micromass LC–ToF mass spectrometer (Wythenshawe, UK) equipped with an electrospray interface. The pumps were programmed to deliver the following gradient at a flow rate of 300 μL min^{-1} (mobile phase A, 5% CH_3CN/95% aqueous ammonium acetate solution (10 mM, pH 7.4); mobile phase B, 95% CH_3CN/5% aqueous ammonium acetate solution (10 mM, pH 7.4)): 100% A (2 min), linear gradient from 100% A to 100% B (2–17 min), 100% B (3 min). Standardized *k'* data were obtained by calibrating against a set of compounds with precisely determined *k'* values (warfarin, testosterone, metoprolol, propranolol, felodipine). The log *D* values in octanol/water are also known for these compounds, which allowed mapping of the results onto a log *D* scale.

c) p*K*a values: The pK_a values were obtained according to reference [37]. The method uses pressure-assisted capillary electrophoresis (HPCE^{3D}, Agilent Technologies) coupled online with an ion trap mass spectrometer (1100 series LC/MSD trap).

d) Solubility in HBSS buffer (pH 7.4): The liquid handling for the solubility assay was automated in a 96-well format using a Multiprobe II HT EX robot (Packard, Meriden, CT, USA). The test substrates (10 μL, 10 mM in DMSO) were diluted with 990 μL of HBSS buffer (pH 7.4) and shaken at room temperature on a flat-bed shaker. After a period of 16 h, samples of 400 μL were filtered

through an 8×12 Whatman GF/B well filter (assisted by vacuum). The filtered samples were analyzed on an Agilent 1100 HPLC system (Waldbronn, Germany) with a diode array detector and coupled to a Micromass LC–ToF mass spectrometer (Wythenshawe, UK) equipped with an electrospray interface. The software used for the evaluation of the data was QuanLynx (Waters). As standards for the concentration estimations, samples with the same degree of dilution were prepared, but with CH_3CN instead of the buffer.

Determination of permeability in a human Caco-2 model

a) Materials: The Caco-2 cells were purchased from ATCC (Rockville, MD, USA). HBSS and HEPES were purchased from GIBCO (Carlsbad, CA, USA), and 2-morpholinoethanesulfonic acid (MES; >99.5%) was purchased from Fluka (Buchs, Switzerland). The water used in the experiments was obtained from a water purification system (Elgastat Maxima, ELGA, Lane End, UK). HBSS buffer (pH 6.5): MES (2.67 g, 13.7 mmol) was dissolved in 500 mL of HBSS, and the pH was adjusted to pH 6.5 by titration with an aqueous solution of NaOH (10 mM). HBSS buffer (pH 7.4): An aqueous solution of HEPES (12.5 mL, 1 M) was added to 500 mL HBSS, and the pH was adjusted to pH 7.4 by titration with an aqueous solution of NaOH (10 mM).

b) Assay: A monolayer of Caco-2 cells, cultured on semipermeable polycarbonate surfaces in 24-transwell plates (Costar, Cambridge, MA, USA), was used to study the permeability in the apical-to-basolateral direction. The process was automated by a robotic Tecan EVO platform (Männerdorf, Switzerland). HBSS buffer (pH 7.4) was dispensed to the basal side of the monolayer. The assay was initiated by adding the test substrate [10 μM in HBSS buffer (pH 6.5)] to the apical side of the monolayer. Samples were withdrawn before the addition of the test substrate and at 45 and 120 min post-addition of the test substrate. During incubation the transwell plates were placed in a shaking incubator at 37 °C between sampling. The quantitative LC–MS analysis procedure was identical to that for the determination of the metabolic stability in liver microsomes (see below). The peak areas were exported to Excel, with which P_{app} values and recoveries were calculated. By using 22 in-house reference compounds, the correlation curve P_{app} versus the fraction of the oral dose absorbed (f_a) was established. The apparent permeability, P_{app}, was calculated using the following equation:

$$P_{app} = (V_r/C_0)(1/S)(dC/dt) \quad (2)$$

where P_{app} is the apparent permeability, V_r is the volume of medium in the receiver chamber, C_0 is the concentration of the test compound in the donor chamber, S is the surface area of the monolayer, and dC/dt is the linear slope of the drug concentration in the receptor chamber with time after correcting for dilution.

Determination of intrinsic clearance and half-lives in liver microsomes

a) Materials: Human liver microsomes as well as female rat liver microsomes were prepared according to reference [38] and stored as granulates at −78 °C. Nicotinamide adenine dinucleotide phosphate (NADPH, reduced form, tetrasodium salt, 98%) was purchased from Sigma Chemical Company (St. Louis, MO, USA). The potassium phosphate buffer (pH 7.4) and CH_3CN were of analytical grade. The water used in the experiments was obtained from a water purification system (Elgastat Maxima, ELGA, Lane End, UK).

b) Assays: The metabolic stability in human and rat liver microsomes was tested by a substrate depletion method. The liquid handling was automated in a 96-well format using a Tecan Genesis Workstation 200 (Männerdorf, Switzerland) equipped with a Tecan GenMate 96 pipetting robot (Männerdorf, Switzerland). A mixture of microsomes (0.5 (mg protein) mL^{-1}), potassium phosphate buffer (93 mM, pH 7.4), and the test substrate (1 μM) was prepared in the 96-well plates and incubated at 37 °C. The reaction was initiated by addition of the cofactor NADPH (1 mM). Aliquots were withdrawn from the incubation mixture at 0, 3, 7, 15, and 30 min, and the reaction was terminated by precipitation of the proteins with 3.5 parts cold CH_3CN. After centrifugation (20 min, 2900 *g*), the supernatant was diluted with an equal amount of H_2O and then analyzed by LC–MS. The LC system consisted of an Agilent 1100 pump (Waldbronn, Germany) and a CTC HTS PAL injector (Zwingen, Switzerland). A Waters Quattro Ultima triple quadrupole mass spectrometer (Wythenshawe, UK), equipped with an electrospray ion source, was used for quantification by selected reaction monitoring. The peaks in the chromatograms were integrated by Waters QuanLynx software, and the peak areas were exported to Excel, with which log[area] versus time [min] was plotted (XLfit). The rate of compound disappearance over time was calculated from the slope of the line (rate constant k). Both clearance values (CL_{int}) and half-lives ($t_{1/2}$) were calculated from k.

Determination of CYP inhibition

a) Materials: A fluorescence-based method according to reference [39] in 96-well format was used to determine the inhibition of five different CYPs (1A2, 2C9, 2D6, 3A4, and 2C19). Nicotinamide adenine dinucleotide phosphate (NADPH, reduced form, tetrasodium salt, 98%) was purchased from Sigma Chemical Co. (St. Louis, MO, USA). The potassium phosphate buffer (pH 7.4) was of analytical grade. The water used in the experiments was obtained from a water purification system (Elgastat Maxima, ELGA, Lane End, UK). The recombinant human enzymes used were prepared in house,[40] except for CYP2D6, which was purchased from CYPEX. The following coumarin substrates, biotransformed into fluorescent metabolites, were used as probes for each individual CYP: CYP1A2, 3-cyano-7-ethoxycoumarin [CEC] (Molecular Probes, Eugene, OR, USA); CYP2C9 and CYP2C19, 7-methoxy-4-(trifluoromethyl)coumarin [MFC] (Sigma Chemical Co., St. Louis, MO, USA); CYP2D6, 7-methoxy-4-(aminomethyl)coumarin [MAMC] (Gentest, Woburn, MA, USA); and CYP3A4, 7-benzyloxy-4-(trifluoromethyl)coumarin [BFC] (Gentest, Woburn, MA, USA). A fluorescence plate reader (SpectraMax GeminiXS, Molecular Devices, Sunnyvale, CA, USA) was used to measure the levels of metabolites formed.

b) Assays: Dilution series of the test substrates were prepared at eight different concentrations (for CYP1A2, CYP2C9, CYP2C19, and CYP2D6: 20.0, 6.67, 2.22, 0.741, 0.247, 0.0823, 0.0274, and 0.00914 μM; for CYP3A4: 50.0, 16.7, 5.56, 1.85, 0.617, 0.206, 0.0686, and 0.0229 μM). For each CYP, a mixture of the enzyme, the corresponding coumarin substrate, potassium phosphate buffer (pH 7.4), and H_2O (concentrations and volumes were CYP-dependent) were added to each well in a black 96-well plate. The test substrates at different concentrations were added. After 10 min pre-incubation, the cofactor NADPH was added to initiate the reaction. After 20–50 min (CYP- and substrate-dependent) the reaction was terminated by the addition of 0.1 M Tris base in 80% CH_3CN/20% H_2O. The plates were transferred to the fluorescence plate reader where the wavelengths were set individually for the different coumarin substrates and their respective fluorescent metabolite (CYP1A2, 3-cyano-7-hydroxycoumarin [CHC]; CYP2C9, CYP2C19,

and CYP3A4, 7-hydroxy-4-(trifluoromethyl)coumarin [HFC]; CYP2D6, 7-hydroxy-4-(aminomethyl)coumarin [HAMC]). The responses were exported to Excel, with which the IC_{50} curves (XLfit) were plotted (percent inhibition versus concentration) and IC_{50} values were calculated for each test substrate and enzyme. For further experimental details of the CYP inhibition assays, see Table 8.

Table 8. Incubation conditions for the CYP inhibition assays.

CYP Enzyme	CYP1A2	CYP2C9	CYP2C19	CYP2D6	CYP3A4
Amount of enzyme [pmol well^{-1}]	1	3	5	6	2
Substrate	CEC	MFC	MFC	MAMC	BFC
Substrate concentration [μM]	3	50	75	15	13
Responsive fluorescent metabolite	CHC	HFC	HFC	HAMC	HFC
Potassium phosphate buffer (pH 7.4) [M]	0.1	0.025	0.05	0.1	0.2
NADPH concentration [mM]	1	1	1	0.4	1
Time of incubation [min]	20	50	40	30	30
Excitation wavelength [nm]	405	405	405	390	405
Emission wavelength [nm]	460	535	535	460	535

Identification of the major in vitro metabolites of sila-haloperidol

The experimental setup for metabolite identification in human liver microsomes was the same as for the determination of the metabolic stability in liver microsomes, with the following modifications: The test substrate concentration was 2 μM, and the reaction was stopped by addition of cold CH_3CN (1:1). A sample corresponding to the half-life of the test compound, determined in the metabolic stability assay, was selected for analysis. In addition, a blank sample without test substrate was analyzed. The samples were analyzed by ultra-performance liquid chromatography (Waters ACQUITY UPLC, Milford, MA, USA) coupled to a Waters Quattro Premier ToF instrument (Wythenshawe, UK) equipped with an electrospray interface. The software used to process the data was MetaboLynx (Waters). Product ion spectra of major metabolites were acquired to allow interpretation and structural assignments.

Supporting information available: Tables of atomic coordinates and equivalent isotropic displacement parameters, anisotropic displacement parameters, experimental details of the X-ray diffraction studies, and bond lengths and angles for **5** and **6**. This material is available free of charge via the internet at http://www.chemmedchem.org. In addition, crystallographic data (excluding structure factors) for the structures reported in this paper have been deposited with the Cambridge Crystallographic Data Centre as supplementary publication nos. CCDC-661268 (**5**) and CCDC-661269 (**6**). These data can be obtained free of charge from The Cambridge Crystallographic Data Centre via www.ccdc.cam.ac.uk/data_request.cif.

Acknowledgements

The following members of the Lead Generation DMPK and Physical Chemistry Section at AstraZeneca R&D Mölndal, Sweden, are gratefully acknowledged for work on physicochemical properties, permeability, and intrinsic clearance: Andreas Landin, Bo Lindmark, Helena Toreson, Johan Wernevik, Hong Wan, Linda Fredlund, Siavash Tavakoli, Birgitta Parkner, David Hansson, Eva Emmanuelsson, Marie Friberg, Anna Schantz Zackrisson, and Walter Lindberg.

Keywords: σ receptors · dopamine receptors · metabolic fate · sila-drugs · silicon

[1] a) P. A. J. Janssen, C. van de Westeringh, A. H. M. Jageneau, P. J. A. Demoen, B. K. F. Hermans, G. H. P. van Daele, K. H. L. Schellekens, C. A. M. van der Eycken, C. J. E. Niemegeers, *J. Med. Pharm. Chem.* **1959**, *1*, 281–297; b) A. P. Holstein, C. H. Chen, *Am. J. Psychiatry* **1965**, *122*, 462–463.

[2] a) B. Capuano, I. T. Crosby, E. J. Lloyd, *Curr. Med. Chem.* **2002**, *9*, 521–548; b) R. Freedman, *N. Engl. J. Med.* **2003**, *349*, 1738–1749.

[3] M. Lyles-Eggleston, R. Altundas, J. Xia, D. M. N. Sikazwe, P. Fan, Q. Yang, S. Li, W. Zhang, X. Zhu, A. W. Schmidt, M. Vanase-Frawley, A. Shrihkande, A. Villalobos, R. F. Borne, S. Y. Ablordeppey, *J. Med. Chem.* **2004**, *47*, 497–508.

[4] Recent reviews dealing with sila-substitution in drug design: a) W. Bains, R. Tacke, *Curr. Opin. Drug Discovery Dev.* **2003**, *6*, 526–543; b) G. A. Showell, J. S. Mills, *Drug Discovery Today* **2003**, *8*, 551–556; c) J. S. Mills, G. A. Showell, *Expert Opin. Invest. Drugs* **2004**, *13*, 1149–1157; d) P. Englebienne, A. van Hoonacker, C. V. Herst, *Drug Des. Rev.–Online* **2005**, *2*, 467–483.

[5] a) R. Tacke, T. Heinrich, R. Bertermann, C. Burschka, A. Hamacher, M. U. Kassack, *Organometallics* **2004**, *23*, 4468–4477; b) R. Tacke, T. Heinrich (Amedis Pharmaceuticals Ltd., UK), UK Patent Appl. GB 2382575A (June 4, **2003**).

[6] Recent original publications dealing with sila-substituted drugs: a) J. O. Daiss, C. Burschka, J. S. Mills, J. G. Montana, G. A. Showell, I. Fleming, C. Gaudon, D. Ivanova, H. Gronemeyer, R. Tacke, *Organometallics* **2005**, *24*, 3192–3199; b) J. O. Daiss, C. Burschka, J. S. Mills, J. G. Montana, G. A. Showell, J. B. H. Warneck, R. Tacke, *Organometallics* **2006**, *25*, 1188–1198; c) G. A. Showell, M. J. Barnes, J. O. Daiss, J. S. Mills, J. G. Montana, R. Tacke, J. B. H. Warneck, *Bioorg. Med. Chem. Lett.* **2006**, *16*, 2555–2558; d) R. Ilg, C. Burschka, D. Schepmann, B. Wünsch, R. Tacke, *Organometallics* **2006**, *25*, 5396–5408; e) M. W. Büttner, C. Burschka, J. O. Daiss, D. Ivanova, N. Rochel, S. Kammerer, C. Peluso-Iltis, A. Bindler, C. Gaudon, P. Germain, D. Moras, H. Gronemeyer, R. Tacke, *ChemBioChem* **2007**, *8*, 1688–1699.

[7] a) J. O. Daiss, M. Penka, C. Burschka, R. Tacke, *Organometallics* **2004**, *23*, 4987–4994; b) J. O. Daiss, K. A. Barth, C. Burschka, P. Hey, R. Ilg, K. Klemm, I. Richter, S. A. Wagner, R. Tacke, *Organometallics* **2004**, *23*, 5193–5197; c) F. Popp, J. B. Nätscher, J. O. Daiss, C. Burschka, R. Tacke, *Organometallics*, in press.

[8] a) S. W. Tam, L. Cook, *Proc. Natl. Acad. Sci. USA* **1984**, *81*, 5618–5621; b) J. M. Walker, W. D. Bowen, F. O. Walker, R. R. Matsumoto, B. De Costa, K. C. Rice, *Pharmacol. Rev.* **1990**, *42*, 355–402.

[9] T. Hayashi, T.-P. Su, *CNS Drugs* **2004**, *18*, 269–284.

[10] a) J. Kim, G. Hewitt, P. Carroll, S. McN. Sieburth, *J. Org. Chem.* **2005**, *70*, 5781–5789; b) D. H. Juers, J. Kim, B. W. Matthews, S. McN. Sieburth, *Biochemistry* **2005**, *44*, 16524–16528; c) S. McN. Sieburth, C.-A. Chen, *Eur. J. Org. Chem.* **2006**, 311–322; d) J. D. Miller, E. D. Baron, H. Scull, A. Hsia, J. C. Berlin, T. McCormick, V. Colussi, M. E. Kenney, K. D. Cooper, N. L. Oleinick, *Toxicol. Appl. Pharmacol.* **2007**, *224*, 290–299.

[11] In this synthesis, approximately 15% bis(4-chlorophenyl)methoxy(2,4,6-trimethoxyphenyl)silane was generated as a byproduct (GC control). The separation of the desired product **4** from this byproduct by distillation was difficult and resulted in low yield for **4**. Aiming at a good yield of **5** in the next step, one may circumvent this problem by synthesizing **5** starting from **2** in a one-pot reaction as described in the Experimental Section under *Method B*.

[12] A. M. Ismaiel, J. de Los Angeles, M. Teitler, S. Ingher, R. A. Glennon, *J. Med. Chem.* **1993**, *36*, 2519–2525.
[13] a) P. J. Kocienski, *Protecting Groups*, Georg Thieme, Stuttgart, **2000**, p. 2; b) T. W. Greene, P. G. M. Wuts, *Protective Groups in Organic Synthesis*, 3rd ed., Wiley, New York, **1999**, p. 1.
[14] D. L. DeHaven-Hudkins, L. C. Fleissner, F. Y. Ford-Rice, *Eur. J. Pharmacol. Mol. Pharmacol. Sect.* **1992**, *227*, 371–378.
[15] a) R. A. Glennon, S. Y. Ablordeppey, A. M. Ismaiel, M. B. El-Ashmawy, J. B. Fischer, K. B. Howie, *J. Med. Chem.* **1994**, *37*, 1214–1219; b) R. A. Glennon, *Mini-Rev. Med. Chem.* **2005**, *5*, 927–940.
[16] F. Yoshida, J. G. Topliss, *J. Med. Chem.* **2000**, *43*, 2575–2585.
[17] P. Baranczewski, A Stańczak, K. Sundberg, R. Svensson, Å. Wallin, J. Jansson, P. Garberg, H. Postlind, *Pharmacol. Rep.* **2006**, *58*, 453–472.
[18] J.-G. Shin, K. Kane, D. A. Flockhart, *Br. J. Clin. Pharmacol.* **2001**, *51*, 45–52.
[19] E. Usuki, R. Pearce, A. Parkinson, N. Castagnoli, Jr., *Chem. Res. Toxicol.* **1996**, *9*, 800–806.
[20] a) J. Gerlach, D. E. Casey, *Acta Psychiatr. Scand.* **1988**, *77*, 369–378; b) H. Kawashima, Y. Iida, Y. Kitamura, H. Saji, *Neurotoxic. Res.* **2004**, *6*, 535–542.
[21] B. Subramanyam, H. Rollema, T. Woolf, N. Castagnoli, Jr., *Biochem. Biophys. Res. Commun.* **1990**, *166*, 238–244.
[22] J. Fang, J. W. Gorrod, *Toxicol. Lett.* **1991**, *59*, 117–123.
[23] B. E. Pape, *J. Anal. Toxicol.* **1981**, *5*, 113–117.
[24] a) K. Chiba, A. Trevor, N. Castagnoli, Jr., *Biochem. Biophys. Res. Commun.* **1984**, *120*, 574–578; b) S. Ottoboni, T. J. Carlson, W. F. Trager, K. Castagnoli, N. Castagnoli, Jr., *Chem. Res. Toxicol.* **1990**, *3*, 423–427.
[25] M. U. Kassack, B. Höfgen, J. Lehmann, N. Eckstein, J. M. Quillan, W. Sadée, *J. Biomol. Screening.* **2002**, *7*, 233–246.
[26] Due to the instability of **7** (elimination of HI), the measured carbon content and hydrogen content both lie above their respective theoretical values.
[27] a) G. M. Sheldrick, SHELXS-97, University of Göttingen, Göttingen, Germany, **1997**; b) G. M. Sheldrick, *Acta Crystallogr. Sect. A* **1990**, *46*, 467–473.
[28] G. M. Sheldrick, SHELXL-97, University of Göttingen, Göttingen, Germany, **1997**.
[29] M. U. Kassack, B. Höfgen, M. Decker, N. Eckstein, J. Lehmann, *Naunyn-Schmiedeberg's Arch. Pharmacol.* **2002**, *366*, 543–550.
[30] M. U. Kassack, *AAPS PharmSci* **2002**, *4*, article 31 (http://www.aapspharmsci.org).
[31] A. DeBlasi, K. O'Reilly, H. J. Motulsky, *Trends Pharmacol. Sci.* **1989**, *10*, 227–229.
[32] M. M. Bradford, *Anal. Biochem.* **1976**, *72*, 248–254.
[33] Y. Cheng, W. H. Prusoff, *Biochem. Pharmacol.* **1973**, *22*, 3099–3108.
[34] C. A. Maier, B. Wünsch, *J. Med. Chem.* **2002**, *45*, 438–448.
[35] S. Bedürftig, B. Wünsch, *Eur. J. Med. Chem.* **2006**, *41*, 387–396.
[36] R. H. Mach, C. R. Smith, S. R. Childers, *Life Sci.* **1995**, *57*, PL57-PL62.
[37] H. Wan, A. G. Holmén, Y. Wang, W. Lindberg, M. Englund, M. B. Någård, R. A. Thompson, *Rapid Commun. Mass Spectrom.* **2003**, *17*, 2639–2648.
[38] L. Ernster, P. Siekevitz, G. E. Palade, *J. Cell Biol.* **1962**, *15*, 541–562.
[39] C. L. Crespi, V. P. Miller, B. W. Penman, *Anal. Biochem.* **1997**, *248*, 188–190.
[40] C. M. Masimirembwa, O. Otter, M. Berg, M. Jönsson, B. Leidvik, E. Jonsson, T. Johansson, A. Bäckman, A. Edlund, T. B. Andersson, *Drug Metab. Dispos.* **1999**, *27*, 1117–1122.

Received: August 10, 2007
Revised: September 24, 2007
Published online on November 19, 2007

